Electronic Supplementary Material (ESI) for Nanoscale.

# Supporting Information

# A highly Crystalline Anthracene-based MOF-74 Series featuring Electrical Conductivity and Luminescence

Patricia I. Scheurle[‡†▽], Andre Mähringer[‡†▽], Andreas C. Jakowetz[†▽], Pouya Hosseini[∞], Alexander F. Richter[▽⊥], Gunther Wittstock[∞], Dana D. Medina[▽†*] and Thomas Bein[▽†*]

[†]Department of Chemistry, Ludwig-Maximilians-Universität (LMU), Butenandtstr. 5-13 (E), 81377 Munich, Germany.

[⊥]Chair for Photonics and Optoelectronics, Nano-Institute Munich, Department of Physics, Ludwig-Maximilians-Universität (LMU), Königinstr. 10, 80539 Munich, Germany.

[▽]Nanosystems Initiative Munich (NIM) and Center for NanoScience (CeNS), Schellingstr. 4, 80799 Munich, Germany.

[∞]Institute of Chemistry, Carl von Ossietzky Universität Oldenburg, 26111 Oldenburg, Germany.

## Table of Contents

## 1. Characterization methods

### Nuclear magnetic resonance (NMR)

NMR spectra were recorded on *Bruker AV400* and *AV400 TR* spectrometers. The chemical shifts are expressed in parts per million and calibrated using residual (undeuterated) solvent peaks as an internal reference ($^1$H-NMR: DMSO-$d_6$: 2.50; $^{13}$C-NMR: DMSO-$d_6$: 39.52). The data for $^1$H-NMR spectra are written as follows: s = singlet, d = doublet, t = triplet, q = quartet, m = multiplet.

### X-ray analysis

X-ray diffraction (XRD) analyses were performed on a *Bruker D8* diffractometer in Bragg-Brentano geometry with Ni-filtered Cu $K_\alpha$ ($\lambda$ = 1.54060 Å) radiation operating at 40 kV and 30 mA with a position-sensitive detector (*LynxEye*).

### Scanning electron microscopy (SEM)

SEM images were recorded on a *FEI Helios NanoLab G3 UC* electron microscope with an acceleration voltage of 2 kV from a field emission gun. For the cross-section analysis substrates were partially cut and broken manually to reveal fresh cross-sections. Prior to SEM analysis the samples were coated with a thin carbon layer by carbon fiber flash evaporation in high vacuum.

### Transmission electron microscopy (TEM)

TEM images were collected on an *FEI Titan Themis 60-300* microscope at an acceleration voltage of 300 kV. Powder samples were prepared by crushing the particles with a razor blade and subsequently depositing the powder onto a copper grid supporting a thin electron transparent carbon film.

## Nitrogen sorption

Ad- and desorption measurements were performed on an *Autosorb 1* (*Quantachrome instruments, Florida, USA*) with nitrogen of 99.9999% purity at 77.3 K. The samples were activated (dried) under high vacuum at 120 °C for at least 12 h. Evaluation of ad- and desorption isotherms was carried out with the *AsiQwin v.3.01* (*Quantachrome instruments, Florida, USA*) software.

For BET calculations, pressure ranges of the nitrogen isotherms were chosen with the help of the BET assistant in the *AsiQwin* software. In accordance with the ISO recommendations, multipoint BET tags equal to or below the maximum in $V \times (1-p/p_0)$ were chosen.

## Van der Pauw measurements

Van der Pauw measurements were conducted on a *ECOPIA Model HMS 3000* Hall measurement setup. The samples were fixed in an *SPCB-1* spring clip board without any additional contacts. Distances between the single probes were adjusted to be 5 mm.

## Preparation of ANMOF-74 and MOF-74 pellets

ANMMOF-74 and MOF-74 pellets with 1 cm diameter (obtained from several described batches) for electrical conductivity measurements were fabricated with 100 mg of the respective MOF bulk material with a standard *Paul-Weber* KBr Press with 45 kg/ $cm^2$ pressure.

## UV-VIS spectroscopy

UV-Vis spectra were recorded using a *PERKIN ELMER UV VIS/NIR Lambda 1050* spectrophotometer equipped with a 150 mm InGaAs integrating sphere. Diffuse reflectance spectra were collected with a Praying Mantis (Harrick) accessory and were referenced to barium sulphate powder as white standard.

## Photoluminescence (PL) spectroscopy

PL measurements were performed on a *PicoQuant FluoTime 300* time-correlated single photon counting (TCSPC) setup. Steady-state spectra and time-resolved histograms were acquired using a 378 nm laser (*PicoQuant LDH-P-C-375*). Residual laser scattering was removed using a 400 nm dielectric long pass (*Thorlabs FELH0400*) in the beam path of the emitted light, which was detected under magic angle (54.7°) on a photomultiplying tube (*PicoQuant PMA 192*).

For measuring the absolute photoluminescence quantum yield and CIE-values, we used a *Horiba FluoroLog 3* in combination with an integrating sphere by *Horiba*. The sample was prepared as follows: a small amount of powder of the MOF was sandwiched between two glass coverslips and sealed using Parafilm at the edges. A reference structure without sample was prepared as well. By relating the signal area change between sample and reference at the luminescence region and at the Rayleigh peak the absolute radiative quantum yield was calculated.

## Thermogravimetric analysis

Thermogravimetric analysis (TGA) measurements were performed on a *Netzsch Jupiter ST 449 C* instrument equipped with a *Netzsch TASC 414/4* controller. The samples were heated from room temperature to 800 °C under a synthetic air flow (25 mL min$^{-1}$) at a heating rate of 1 K min$^{-1}$.

## X-ray photoelectron spectroscopy

XPS was performed using an ESCALAB 250 Xi instrument (Thermo Fisher, East Grinsted, UK) with monochromatized Al Kα (hν = 1486.6 eV) radiation focused to a spot of 500 micron diameter at the surface of samples. Spectra were measured with pass energies of 200 eV for survey scans and 10 eV for high-resolution regions. Charging was compensated by use of an internal electron flood gun. Peak fitting was performed by the software Avantage, version 5.9904 (Thermo Fisher) using a Shirley background (“Smart Shirley”) and a convolution of Gaussian and Lorentzian functions for each signal component. All spectra were referenced to remaining adventitious carbon at 284.8 eV.

## Elemental Analysis

The elemental analysis for carbon and hydrogen for ANMOF-74 (M) was performed on a Vario MICRO cube instrument (Elementar Analysensysteme GmbH, Germany). The metal detection for all samples was carried out on a Varian Vista RL ICP-OES spectrometer. All materials were treated under dynamic vacuum prior to analysis.

## 2. Experimental

### General

All materials were purchased from *Sigma Aldrich, Acros or TCI Europe* in the common purities *purum*, *puriss* or *reagent grade.* The materials were used as received without additional purification and handled in air unless otherwise noted.

The water utilized in the synthesis was subjected to a *Merck-Milipore Mili-Q* purification system prior to use.

### Synthetic procedures

**Methyl 2-hydroxy-4-(4,4,5,5-tetramethyl-1,3,2-dioxaborolan-2-yl)benzoate** (compound **3**) (adapted from Fracaroli, A. M.; Furukawat, H.; Suzuki, M.; Dodd, M.; Okajima, S.; Gandarat, F.; Reimer, J. A.; Yaghi, O. M. *Metal-organic Frameworks with Preciseley Designed Interior for Carbon Dioxide Capture in the Presence of Water. J. Am. Chem. Soc.* **2014,** *136*, 8863–8866.)

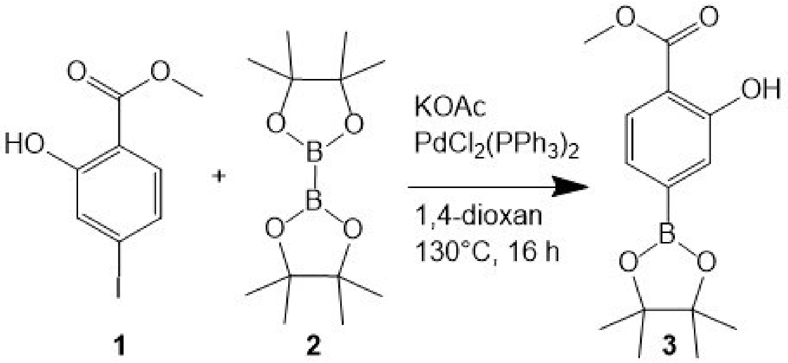

**Scheme S1.**

Methyl 4-iodosalicylate (compound **1**) (1.0 g, 3.6 mmol), bis(pinacolato)diboron (compound **2**) (1.01 g, 3.98 mmol), KOAc (1.1 g, 10.8 mmol), and $PdCl_2(PPh_3)_2$ (50.7 mg, 0.072 mmol) were dissolved in 18 mL anhydrous 1,4-dioxane in a 100 mL flask under nitrogen atmosphere. The resulting solution was heated to 130 °C for 13 h under stirring. The solution was allowed to cool to room temperature and filtered through celite. It was washed with 1,4-dioxane, toluene and ethyl acetate. The filtrate was concentrated in vacuo. The obtained yellow solid was dissolved in ethyl acetate. The white solid was filtered off. The filtrate was concentrated under vacuum. The obtained yellow needles were recrystallized in methanol (2 mL), giving colorless crystals with 71% yield. $^1H$ NMR (400 MHz, DMSO-$d_6$) δ (ppm): 10.35 (s, 1H), 7.75 (d, 1H) 7.20 (s, 1H), 7.17 (d, 1H), 3.87 (s, 3 H), 1.26 (s, 12H).

**Dimethyl 4,4´-(anthracene-9,10-diyl)bis(2-hydroxybenzoate)** (compound **5**) (adapted from Hirofumi M., Akira S., Yusuke M., Yoshinori I. Polycarboxylic acid containing condensed aromatic ring, crystalline network complex using same, and gas storage material. **2017**. WO 2017006638 A1.)

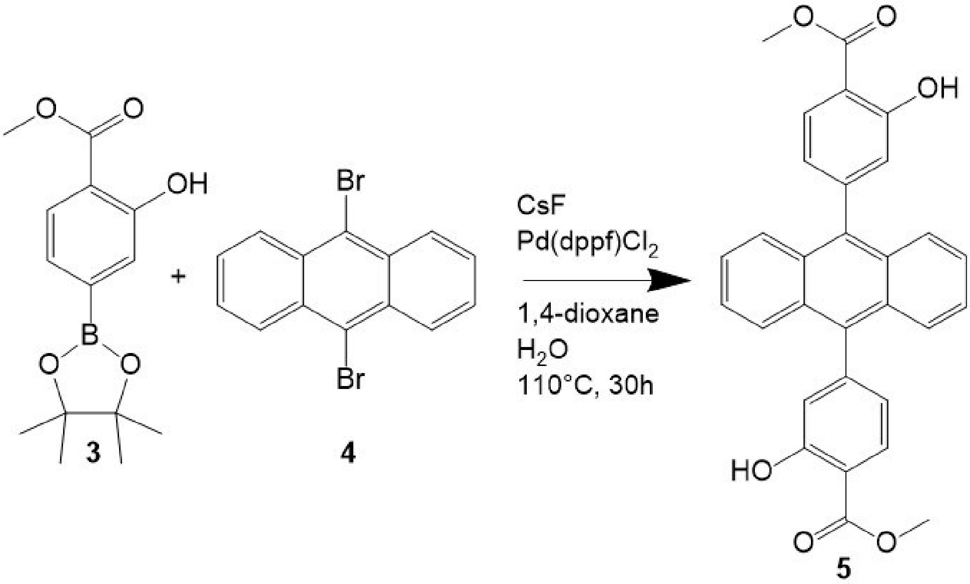

**Scheme S2.**

Methyl 2-hydroxy-4-(4,4,5,5-tetramethyl-1,3,2-dioxaborolan-2-yl)benzoate (compound **3**) (700 mg, 2.5 mmol), 9,10-dibromoanthracene (compound **4**) (369 mg, 1.099 mmol), CsF (1.0 g, 65.8 µmol), Pd(dppf)$Cl_2$ (44.85 mg, 613 µmol) were dissolved in 12.8 mL 1,4-dioxane and 1.8 mL water in a 100 mL flask under nitrogen atmosphere. The resulting solution was heated to 110 °C for 30 h. The solution was allowed to cool to room temperature and $NH_4Cl$ (40 mL) and chloroform (40 mL) were added. It was filtered through celite and the residue was washed with chloroform (400 mL). The filtrate was separated and the aqueous layer was extracted with chloroform. The organic layer was washed with saturated sodium chloride solution (3 x 200 mL) and dried over $MgSO_4$. The filtrate was concentrated under vacuum, giving a brown powder with 72% yield. $^1H$ NMR (400 MHz, DMSO-$d_6$) δ (ppm): 8.04 (d, 2H), 7.64-7.59 (m, 4H), 7.49-7.45 (m, 4H), 7.09 (t, 2H), 7.06-7.03 (ddd, 2H), 3.99 (s, 6H).

**4,4´-(anthracene-9,10-diyl)bis(2-hydroxybenzoic acid)** (compound **6**) ABHB linker, (adapted from Hirofumi M., Akira S., Yusuke M., Yoshinori I. (2017). WO 2017006638 A1.)

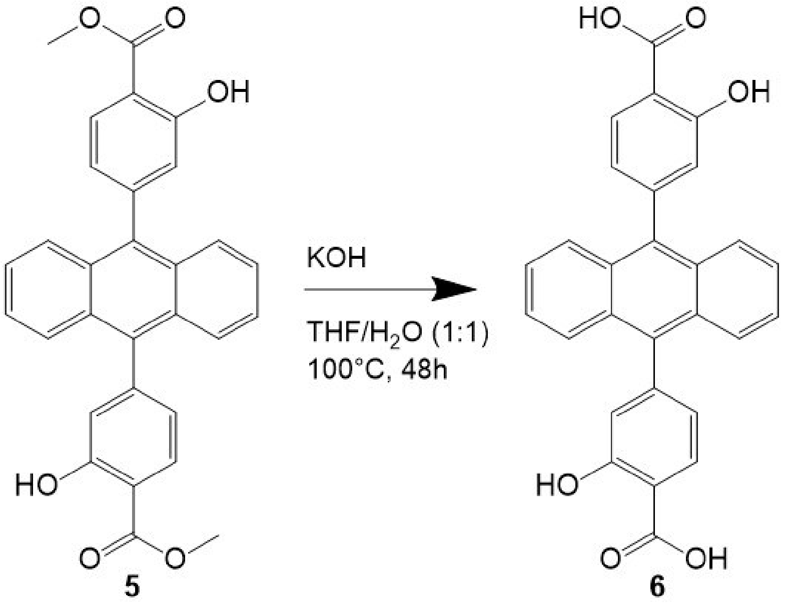

**Scheme S3.**

Dimethyl 4,4´-(anthracene-9,10-diyl)bis(2-hydroxybenzoate) (compound **5**) (300 mg, 0.63 mmol), potassium hydroxide (KOH) (500 mg, 8.9 mmol) and a mixture of THF/$H_2O$ (1:1) (30 mL) were heated in a 100 mL flask under nitrogen atmosphere at 100 °C for 48 h. The resulting solution was allowed to cool to room temperature and poured into HCl (200 mL). The solid was filtered off, washed with acetic acid (30 mL), water (500 mL) and MeOH (30 mL) and dried under vacuum, giving a beige powder with 70% yield. $^1$H NMR (400 MHz, DMSO-$d_6$) δ (ppm): 8.03 (d, 2H), 7.64-7.59 (m, 4H), 7.48-7.43 (m, 4H), 7.03 (s, 2H), 7.02-6.97 (m, 2H), 3.99 (s, 6H). $^{13}$C NMR (400 MHz, DMSO-$d_6$) δ (ppm): 171.73 (2C), 161.07 (2C), 145.75 (2C), 135.59 (2C), 130.60 (3C), 128.51 (3C), 126.13 (6C), 125.92 (3C), 122.11 (4C).

## Anthracene-based MOF-74 (ANMOF-74) synthesis

### ANMOF-74(Zn)

4,4´-(anthracene-9,10-diyl)bis(2-hydroxybenzoic acid) (10.00 mg, 0.022 mmol), $Zn(NO_3)_2 \cdot 4H_2O$ (22.07 mg, 0.084 mmol) and benzoic acid (2.7 mg, 0.022 mmol) were suspended in DMF (1.5 mL). The resulting mixture was sonicated until complete dissolution of the educts was achieved and it was kept in a culture tube at 120 °C for 2 days. The resulting precipitate was washed with DMF (2 x 10 mL) and MeOH (1 x 10 mL) and activated at 120°C to remove the less volatile solvent to obtain a brownish crystalline powder. The PXRD pattern of the synthesized MOF matches the simulated ANMOF-74 PXRD pattern. Elemental Analysis (vacuum treated): Calculated for $Zn_{18}C_{252}H_{126}O_{63} \cdot$ DMF (%): Zn, 22.04; C, 56.70; H. 2.38; Found (%): Zn, 21.48; C, 56.91; H, 2.57, N, 0.71.

### ANMOF-74(Mg)

4,4´-(anthracene-9,10-diyl)bis(2-hydroxybenzoic acid) (10.00 mg, 0.022 mmol) and $Mg(NO_3)_2 \cdot 6H_2O$ (21.60 mg, 0.084 mmol) were suspended in DMF (1.3 mL) and MeOH (0.2 mL). The resulting mixture was sonicated until complete dissolution of the educts was achieved and it was kept in a culture tube at 120°C for 2 days. The resulting precipitate was washed with DMF (2 x 10 mL) and MeOH (1 x 10 mL) and activated at 120 °C to remove the less volatile solvent to obtain a bright beige crystalline powder. The PXRD pattern of the synthesized MOF matches the simulated ANMOF-74 PXRD pattern. Elemental Analysis (vacuum treated): Calculated for $Mg_{18}C_{252}H_{126}O_{63} \cdot$ DMF (%): Mg, 9.51; C, 65.81; H, 2.76; Found (%): Mg, 9.12; C, 66.12; H, 2.97, N, 0.59.

### ANMOF-74(Ni)

4,4´-(anthracene-9,10-diyl)bis(2-hydroxybenzoic acid) (10.00 mg, 0.022 mmol), $NiCl_2$ (10.80 mg, 0.084 mmol) and benzoic acid (2.7 mg, 0.022 mmol) were suspended in benzyl alcohol (0.7 mL) and EtOH (0.7 mL) The resulting mixture was sonicated until complete dissolution of the educts was achieved and it was kept in a culture tube at 120 C for 2 days. The resulting precipitate was washed with DMF (2 x 10 mL) and MeOH (1 x 10 mL) and activated at 120°C to remove the less volatile solvent to obtain a green crystalline powder.

The PXRD pattern of the synthesized MOF matches the simulated ANMOF-74 PXRD pattern. Elemental Analysis (vacuum treated): Calculated for $Ni_{18}C_{252}H_{126}O_{63}$ · DMF (%): Ni, 20.25; C, 58.00; H. 2.43; Found (%): Ni, 19.37; C, 58.84; H, 2.60, N 0.61.

### ANMOF-74(Co)

4,4´-(anthracene-9,10-diyl)bis(2-hydroxybenzoic acid) (10.00 mg, 0.022 mmol), $Co(NO_3)_2 \cdot 6H_2O$ (24.30 mg, 0.084 mmol) and benzoic acid (2.7 mg, 0.022 mmol) were suspended in DMF (1.1 mL), EtOH (0.3 mL) and $H_2O$ (1 mL). The resulting mixture was sonicated until complete dissolution of the educts was achieved and it was kept in a culture tube at 120 C for 2 days. The resulting precipitate was washed with DMF (2 x 10 mL) and MeOH (1 x 10 mL) and activated at 120 °C to remove the less volatile solvent to obtain a pink crystalline powder. The PXRD pattern of the synthesized MOF matches the simulated ANMOF-74 PXRD pattern. Elemental Analysis (vacuum treated): Calculated for $Co_{18}C_{252}H_{126}O_{63}$ · DMF (%): Co, 20.31; C, 57.96; H. 2.43; Found (%): Co, 19.78; C, 58.16; H, 2.79, N, 0.65.

### ANMOF-74(Mn)

4,4´-(anthracene-9,10-diyl)bis(2-hydroxybenzoic acid) (10.00 mg, 0.022 mmol) and $MnCl_2 \cdot 4H_2O$ (22.60 mg, 0.084 mmol) were suspended in DMF (1.5 mL). The resulting mixture was sonicated until complete dissolution of the educts was achieved and it was kept in a culture tube at 120°C for 2 days. The resulting precipitate was washed with DMF (2 x 10 mL) and MeOH (1 x 10 mL) and activated at 120 °C to remove the less volatile solvent to obtain a light beige crystalline powder. The PXRD pattern of the synthesized MOF matches the simulated ANMOF-74 PXRD pattern. Elemental Analysis (vacuum treated): Calculated for $Mn_{18}C_{252}H_{126}O_{63}$ · DMF (%): Mn, 19.20; C, 58.77; H. 2.47; Found (%): Mn, 18.07; C, 58.94, H, 2.67, N, 0.56.

## MOF-74 synthesis

### MOF-74(Zn)

The synthesis was adapted from: Rosi, N. L.; Kim, J.; Eddaoudi, M.; Chen, B.; O´Keeffe, M.; Yaghi, O. M. Rod Packings and metal-Organic Frameworks Constructed from Rod-Shaped Secondary Building Units. *J. Am. Chem. Soc.* **2005**, *127*, 1504-1518.

2,5-dihydroxy-1,4-benzenedicarboxylic acid (0.019 g, 0.096 mmol) and zinc nitrate tetrahydrate, $Zn(NO_3)_2{\cdot}4H_2O$ (0.053 mg, 0.203 mmol) were dissolved in DMF (2 mL), 2-propanol (0.1 mL) and water (0.1 mL). The resulting mixture was sonicated until complete dissolution of the educts was achieved and it was kept in a culture tube at 105°C for 1 day. The resulting precipitate was washed with DMF (2 x 10 mL) and ethanol (1 x 10 mL) and dried under reduced pressure.

**MOF-74(Mg)**

The synthesis was adapted from: Caskey, S. R.; Wong-Foy, A. G.; Matzger, A. J. Dramatic Tuning of Carbon Dioxide Uptake via Metal Substitution in a Coordination Polymer with Cylindrical Pores. *J. Am. Chem. Soc.* **2008**, *130*, 18070-18071.

2,5-dihydroxy-1,4-benzenedicarboxylic acid (0.111 g, 0.559 mmol) and magnesia nitrate hexahydrate, $Mg(NO_3)_2{\cdot}6H_2O$ (0.475 mg, 1.85 mmol) were dissolved in a 15:1:1 mixture of DMF-ethanol-water (50 mL). The resulting mixture was sonicated until complete dissolution of the educts was achieved and it was kept in a Teflon sealed 100 mL Schott Duran glass bottle at 125°C for 1 day. The resulting precipitate was washed with DMF (2 x 10 mL) and methanol (1 x 10 mL) and dried under reduced pressure.

**MOF-74(Ni)**

The synthesis was adapted from: Caskey, S. R.; Wong-Foy, A. G.; Matzger, A. J. Dramatic Tuning of Carbon Dioxide Uptake via Metal Substitution in a Coordination Polymer with Cylindrical Pores. *J. Am. Chem. Soc.* **2008**, *130*, 18070-18071.

2,5-dihydroxy-1,4-benzenedicarboxylic acid (0.478 g, 2.41 mmol) and nickel nitrate hexahydrate, $Ni(NO_3)_2{\cdot}6H_2O$ (2.378 mg, 8.178 mmol) were dissolved in a 1:1:1 mixture of DMF-ethanol-water (200 mL). The resulting mixture was sonicated until complete dissolution of the educts was achieved and it was kept in three Teflon sealed 100 mL Schott Duran glass bottles at 100°C for 1 day. The resulting precipitate was washed with DMF (2 x 10 mL) and methanol (1 x 10 mL) and dried under reduced pressure.

**MOF-74(Co)**

The synthesis was adapted from: Caskey, S. R.; Wong-Foy, A. G.; Matzger, A. J. Dramatic Tuning of Carbon Dioxide Uptake via Metal Substitution in a Coordination Polymer with Cylindrical Pores. *J. Am. Chem. Soc.* **2008**, *130*, 18070-18071.

2,5-dihydroxy-1,4-benzenedicarboxylic acid (0.482 g, 2.43 mmol) and cobalt nitrate hexahydrate, $Co(NO_3)_2 \cdot 6H_2O$ (2.377 g, 8.67 mmol) were dissolved in a 1:1:1 mixture of DMF-ethanol-water (200 mL). The resulting mixture was sonicated until complete dissolution of the educts was achieved and it was kept in three Teflon sealed 100 mL Schott Duran glass bottles at 100°C for 1 day. The resulting precipitate was washed with DMF (2 x 10 mL) and methanol (1 x 10 mL) and dried under reduced pressure.

**MOF-74(Mn)**

The synthesis was adapted from: Cozzolino, A. F.; Brozek, A. K., Palmer, R. D.; Yano, J.; Li, Minyuan; Dinca, M. Ligand Redox Non-Innocence in the Stoichiometric Oxidation of $Mn_2$(2,5-dioxidoterephtalate) (Mn-MOF-74). *J. Am. Chem. Soc.* **2014**, *136*, 3334-3337.

2,5-dihydroxy-1,4-benzenedicarboxylic acid (0.27 g, 1.3 mmol) and $MnCl_2 \cdot 4H_2O$ (1.07 g, 5.41 mmol) were dissolved in a 15:1 mixture of DMF-ethanol (32 mL) under argon atmosphere. The resulting mixture was sonicated until complete dissolution of the educts was achieved and it was kept in a Teflon sealed 100 mL Schott Duran glass bottle at 135°C for 3 day. The resulting precipitate was washed with DMF (2 x 10 mL) and methanol (1 x 10 mL) and dried under reduced pressure.

# 3. Characterization

## Unit cell parameters and atomic coordinates

### ANMOF-74(Zn)

$R_{wp}$ = 6.74%, $R_p$ = 4.99%

| |
|---|
| R*3* (146) - trigonal |
| a = b = 46.06 Å, c = 5.78 Å |
| α = β = 90°, γ = 120° |

| **Atom** | **x/a** | **y/b** | **z/c** |
|---|---|---|---|
| O1 | 0.6465 | 0.6054 | -0.1318 |
| O2 | 0.6262 | 0.6377 | 0.0040 |
| O3 | 0.6388 | 0.6434 | 0.4834 |
| O4 | 0.3912 | 0.3476 | 1.6885 |
| O5 | 0.3647 | 0.3616 | 0.9242 |
| O6 | 0.3606 | 0.3515 | 1.3502 |
| Zn7 | 0.6542 | 0.6711 | 0.1483 |
| O8 | 0.3593 | 0.389 | 1.5693 |
| Zn9 | 0.3506 | 0.3453 | 1.6414 |
| C10 | 0.6163 | 0.6077 | 0.4376 |
| C11 | 0.5890 | 0.5870 | 0.5889 |
| C12 | 0.5687 | 0.5518 | 0.5495 |
| C13 | 0.5772 | 0.5377 | 0.3678 |
| C14 | 0.6015 | 0.5577 | 0.2096 |
| C15 | 0.4166 | 0.4155 | 0.8479 |
| C16 | 0.3885 | 0.3933 | 0.9881 |
| C17 | 0.4051 | 0.4386 | 1.2642 |
| C18 | 0.4312 | 0.4604 | 1.1229 |
| C19 | 0.4385 | 0.4493 | 0.9190 |
| C20 | 0.4709 | 0.4741 | 0.8078 |
| C21 | 0.5002 | 0.4726 | 0.8493 |
| C22 | 0.5323 | 0.4991 | 0.7803 |
| C23 | 0.5361 | 0.5282 | 0.6700 |
| C24 | 0.5068 | 0.5299 | 0.6302 |
| C25 | 0.4747 | 0.5033 | 0.6996 |
| C26 | 0.4464 | 0.5063 | 0.6562 |
| C27 | 0.4493 | 0.5342 | 0.5447 |
| C28 | 0.4804 | 0.5598 | 0.4744 |

| | | | |
|---|---|---|---|
| C29 | 0.5088 | 0.5576 | 0.5165 |
| C30 | 0.5605 | 0.4961 | 0.8249 |
| C31 | 0.5577 | 0.4681 | 0.9369 |
| C32 | 0.5265 | 0.4426 | 1.0065 |
| C33 | 0.4981 | 0.4448 | 0.9632 |
| C34 | 0.6286 | 0.6102 | 0.0372 |
| C35 | 0.6180 | 0.5924 | 0.2302 |
| C36 | 0.3671 | 0.3823 | 1.3633 |
| C37 | 0.3853 | 0.4053 | 1.1998 |

**ANMOF-74(Mg)**

$R_{wp}$ = 6.96%, $R_p$ = 5.16%

| |
|---|
| R*3* (146) - trigonal |
| a = b = 46.36 Å, c = 6.05 Å |
| α = β = 90°, γ = 120° |

| **Atom** | **x/a** | **y/b** | **z/c** |
|---|---|---|---|
| O1 | 0.6465 | 0.6054 | -0.1318 |
| O2 | 0.6262 | 0.6377 | 0.0040 |
| O3 | 0.6388 | 0.6434 | 0.4834 |
| O4 | 0.3912 | 0.3476 | 1.6885 |
| O5 | 0.3647 | 0.3616 | 0.9242 |
| O6 | 0.3606 | 0.3515 | 1.3502 |
| Mg7 | 0.6542 | 0.6711 | 0.1483 |
| O8 | 0.3593 | 0.389 | 1.5693 |
| Mg9 | 0.3506 | 0.3453 | 1.6414 |
| C10 | 0.6163 | 0.6077 | 0.4376 |
| C11 | 0.5890 | 0.5870 | 0.5889 |
| C12 | 0.5687 | 0.5518 | 0.5495 |
| C13 | 0.5772 | 0.5377 | 0.3678 |
| C14 | 0.6015 | 0.5577 | 0.2096 |
| C15 | 0.4166 | 0.4155 | 0.8479 |
| C16 | 0.3885 | 0.3933 | 0.9881 |
| C17 | 0.4051 | 0.4386 | 1.2642 |
| C18 | 0.4312 | 0.4604 | 1.1229 |
| C19 | 0.4385 | 0.4493 | 0.9190 |
| C20 | 0.4709 | 0.4741 | 0.8078 |
| C21 | 0.5002 | 0.4726 | 0.8493 |

| | | | |
|---|---|---|---|
| C22 | 0.5323 | 0.4991 | 0.7803 |
| C23 | 0.5361 | 0.5282 | 0.6700 |
| C24 | 0.5068 | 0.5299 | 0.6302 |
| C25 | 0.4747 | 0.5033 | 0.6996 |
| C26 | 0.4464 | 0.5063 | 0.6562 |
| C27 | 0.4493 | 0.5342 | 0.5447 |
| C28 | 0.4804 | 0.5598 | 0.4744 |
| C29 | 0.5088 | 0.5576 | 0.5165 |
| C30 | 0.5605 | 0.4961 | 0.8249 |
| C31 | 0.5577 | 0.4681 | 0.9369 |
| C32 | 0.5265 | 0.4426 | 1.0065 |
| C33 | 0.4981 | 0.4448 | 0.9632 |
| C34 | 0.6286 | 0.6102 | 0.0372 |
| C35 | 0.6180 | 0.5924 | 0.2302 |
| C36 | 0.3671 | 0.3823 | 1.3633 |
| C37 | 0.3853 | 0.4053 | 1.1998 |

**ANMOF-74(Ni)**

$R_{wp}$ = 3.94%, $R_p$ = 3.15%

| |
|---|
| R*3* (146) - trigonal |
| a = b = 46.21 Å, c = 5.76 Å |
| α = β = 90°, γ = 120° |

| **Atom** | **x/a** | **y/b** | **z/c** |
|---|---|---|---|
| O1 | 0.6465 | 0.6054 | -0.1318 |
| O2 | 0.6262 | 0.6377 | 0.0040 |
| O3 | 0.6388 | 0.6434 | 0.4834 |
| O4 | 0.3912 | 0.3476 | 1.6885 |
| O5 | 0.3647 | 0.3616 | 0.9242 |
| O6 | 0.3606 | 0.3515 | 1.3502 |
| Ni7 | 0.6542 | 0.6711 | 0.1483 |
| O8 | 0.3593 | 0.389 | 1.5693 |
| Ni9 | 0.3506 | 0.3453 | 1.6414 |
| C10 | 0.6163 | 0.6077 | 0.4376 |
| C11 | 0.5890 | 0.5870 | 0.5889 |
| C12 | 0.5687 | 0.5518 | 0.5495 |
| C13 | 0.5772 | 0.5377 | 0.3678 |
| C14 | 0.6015 | 0.5577 | 0.2096 |

| | | | |
|---|---|---|---|
| C15 | 0.4166 | 0.4155 | 0.8479 |
| C16 | 0.3885 | 0.3933 | 0.9881 |
| C17 | 0.4051 | 0.4386 | 1.2642 |
| C18 | 0.4312 | 0.4604 | 1.1229 |
| C19 | 0.4385 | 0.4493 | 0.9190 |
| C20 | 0.4709 | 0.4741 | 0.8078 |
| C21 | 0.5002 | 0.4726 | 0.8493 |
| C22 | 0.5323 | 0.4991 | 0.7803 |
| C23 | 0.5361 | 0.5282 | 0.6700 |
| C24 | 0.5068 | 0.5299 | 0.6302 |
| C25 | 0.4747 | 0.5033 | 0.6996 |
| C26 | 0.4464 | 0.5063 | 0.6562 |
| C27 | 0.4493 | 0.5342 | 0.5447 |
| C28 | 0.4804 | 0.5598 | 0.4744 |
| C29 | 0.5088 | 0.5576 | 0.5165 |
| C30 | 0.5605 | 0.4961 | 0.8249 |
| C31 | 0.5577 | 0.4681 | 0.9369 |
| C32 | 0.5265 | 0.4426 | 1.0065 |
| C33 | 0.4981 | 0.4448 | 0.9632 |
| C34 | 0.6286 | 0.6102 | 0.0372 |
| C35 | 0.6180 | 0.5924 | 0.2302 |
| C36 | 0.3671 | 0.3823 | 1.3633 |
| C37 | 0.3853 | 0.4053 | 1.1998 |

**ANMOF-74(Co)**

$R_{wp}$ = 4.18%, $R_p$ = 2.55%

| |
|---|
| R*3* (146) - trigonal |
| a = b = 46.11 Å, c = 5.92 Å |
| α = β = 90°, γ = 120° |

| Atom | x/a | y/b | z/c |
|---|---|---|---|
| O1 | 0.6465 | 0.6054 | -0.1318 |
| O2 | 0.6262 | 0.6377 | 0.0040 |
| O3 | 0.6388 | 0.6434 | 0.4834 |
| O4 | 0.3912 | 0.3476 | 1.6885 |
| O5 | 0.3647 | 0.3616 | 0.9242 |
| O6 | 0.3606 | 0.3515 | 1.3502 |
| Co7 | 0.6542 | 0.6711 | 0.1483 |

| | | | |
|---|---|---|---|
| O8 | 0.3593 | 0.389 | 1.5693 |
| Co9 | 0.3506 | 0.3453 | 1.6414 |
| C10 | 0.6163 | 0.6077 | 0.4376 |
| C11 | 0.5890 | 0.5870 | 0.5889 |
| C12 | 0.5687 | 0.5518 | 0.5495 |
| C13 | 0.5772 | 0.5377 | 0.3678 |
| C14 | 0.6015 | 0.5577 | 0.2096 |
| C15 | 0.4166 | 0.4155 | 0.8479 |
| C16 | 0.3885 | 0.3933 | 0.9881 |
| C17 | 0.4051 | 0.4386 | 1.2642 |
| C18 | 0.4312 | 0.4604 | 1.1229 |
| C19 | 0.4385 | 0.4493 | 0.9190 |
| C20 | 0.4709 | 0.4741 | 0.8078 |
| C21 | 0.5002 | 0.4726 | 0.8493 |
| C22 | 0.5323 | 0.4991 | 0.7803 |
| C23 | 0.5361 | 0.5282 | 0.6700 |
| C24 | 0.5068 | 0.5299 | 0.6302 |
| C25 | 0.4747 | 0.5033 | 0.6996 |
| C26 | 0.4464 | 0.5063 | 0.6562 |
| C27 | 0.4493 | 0.5342 | 0.5447 |
| C28 | 0.4804 | 0.5598 | 0.4744 |
| C29 | 0.5088 | 0.5576 | 0.5165 |
| C30 | 0.5605 | 0.4961 | 0.8249 |
| C31 | 0.5577 | 0.4681 | 0.9369 |
| C32 | 0.5265 | 0.4426 | 1.0065 |
| C33 | 0.4981 | 0.4448 | 0.9632 |
| C34 | 0.6286 | 0.6102 | 0.0372 |
| C35 | 0.6180 | 0.5924 | 0.2302 |
| C36 | 0.3671 | 0.3823 | 1.3633 |
| C37 | 0.3853 | 0.4053 | 1.1998 |

**ANMOF-74(Mn)**

$R_{wp}$ = 4.38%, $R_p$ = 2.80%

| |
|---|
| R*3* (146) - trigonal |
| a = b = 46.21 Å, c = 5.69 Å |
| α = β = 90°, γ = 120° |

| **Atom** | **x/a** | **y/b** | **z/c** |
|---|---|---|---|

| | | | |
|---|---|---|---|
| O1 | 0.6465 | 0.6054 | -0.1318 |
| O2 | 0.6262 | 0.6377 | 0.0040 |
| O3 | 0.6388 | 0.6434 | 0.4834 |
| O4 | 0.3912 | 0.3476 | 1.6885 |
| O5 | 0.3647 | 0.3616 | 0.9242 |
| O6 | 0.3606 | 0.3515 | 1.3502 |
| Mn7 | 0.6542 | 0.6711 | 0.1483 |
| O8 | 0.3593 | 0.389 | 1.5693 |
| Mn9 | 0.3506 | 0.3453 | 1.6414 |
| C10 | 0.6163 | 0.6077 | 0.4376 |
| C11 | 0.5890 | 0.5870 | 0.5889 |
| C12 | 0.5687 | 0.5518 | 0.5495 |
| C13 | 0.5772 | 0.5377 | 0.3678 |
| C14 | 0.6015 | 0.5577 | 0.2096 |
| C15 | 0.4166 | 0.4155 | 0.8479 |
| C16 | 0.3885 | 0.3933 | 0.9881 |
| C17 | 0.4051 | 0.4386 | 1.2642 |
| C18 | 0.4312 | 0.4604 | 1.1229 |
| C19 | 0.4385 | 0.4493 | 0.9190 |
| C20 | 0.4709 | 0.4741 | 0.8078 |
| C21 | 0.5002 | 0.4726 | 0.8493 |
| C22 | 0.5323 | 0.4991 | 0.7803 |
| C23 | 0.5361 | 0.5282 | 0.6700 |
| C24 | 0.5068 | 0.5299 | 0.6302 |
| C25 | 0.4747 | 0.5033 | 0.6996 |
| C26 | 0.4464 | 0.5063 | 0.6562 |
| C27 | 0.4493 | 0.5342 | 0.5447 |
| C28 | 0.4804 | 0.5598 | 0.4744 |
| C29 | 0.5088 | 0.5576 | 0.5165 |
| C30 | 0.5605 | 0.4961 | 0.8249 |
| C31 | 0.5577 | 0.4681 | 0.9369 |
| C32 | 0.5265 | 0.4426 | 1.0065 |
| C33 | 0.4981 | 0.4448 | 0.9632 |
| C34 | 0.6286 | 0.6102 | 0.0372 |
| C35 | 0.6180 | 0.5924 | 0.2302 |
| C36 | 0.3671 | 0.3823 | 1.3633 |
| C37 | 0.3853 | 0.4053 | 1.1998 |

## Powder X-ray diffraction

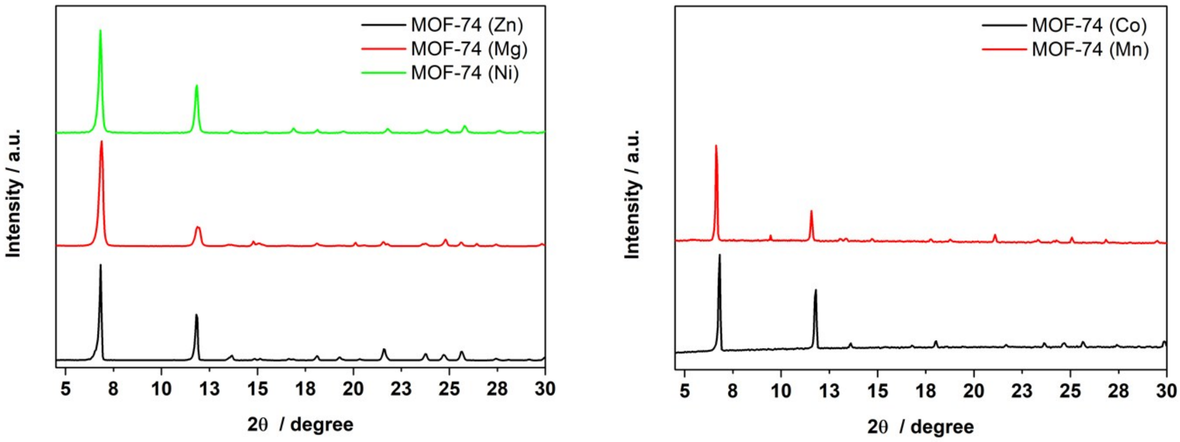

**Figure S1:** PXRD patterns of the MOF-74(M) bulk materials.

## Scanning-electron microscopy

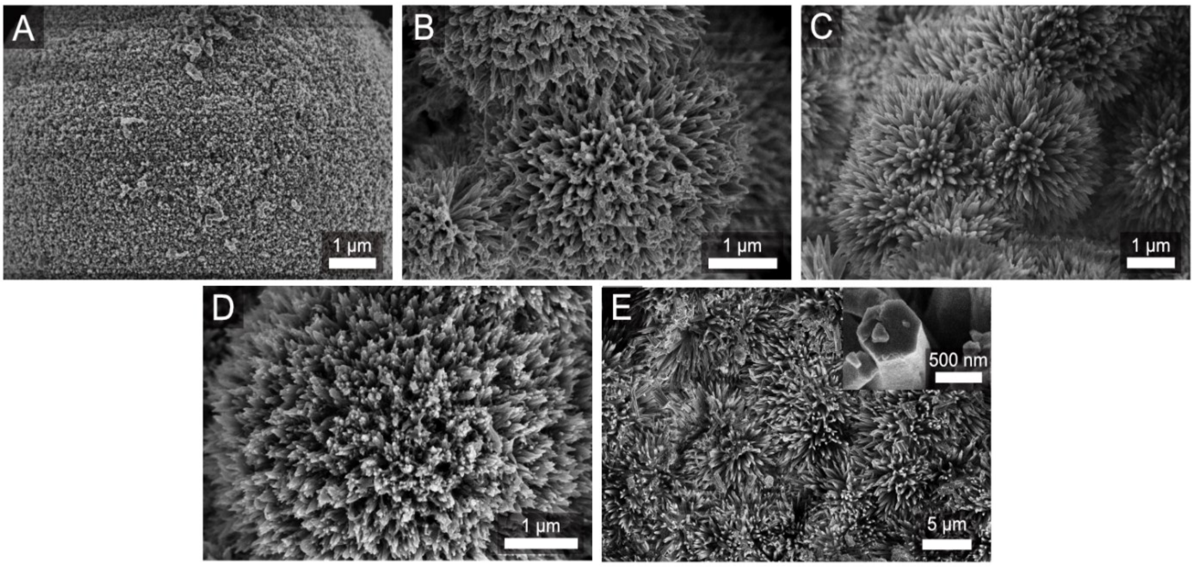

**Figure S2**: SEM images of the ANMOF-74 bulk materials **(A)** ANMOF-74(Zn), **(B)** ANMOF-74(Mg), **(C)** ANMOF-74(Ni), **(D)** ANMOF-74(Co), **(E)** ANMOF-74(Mn) and a close-up of a hexagonally shaped monolith depicted as inset.

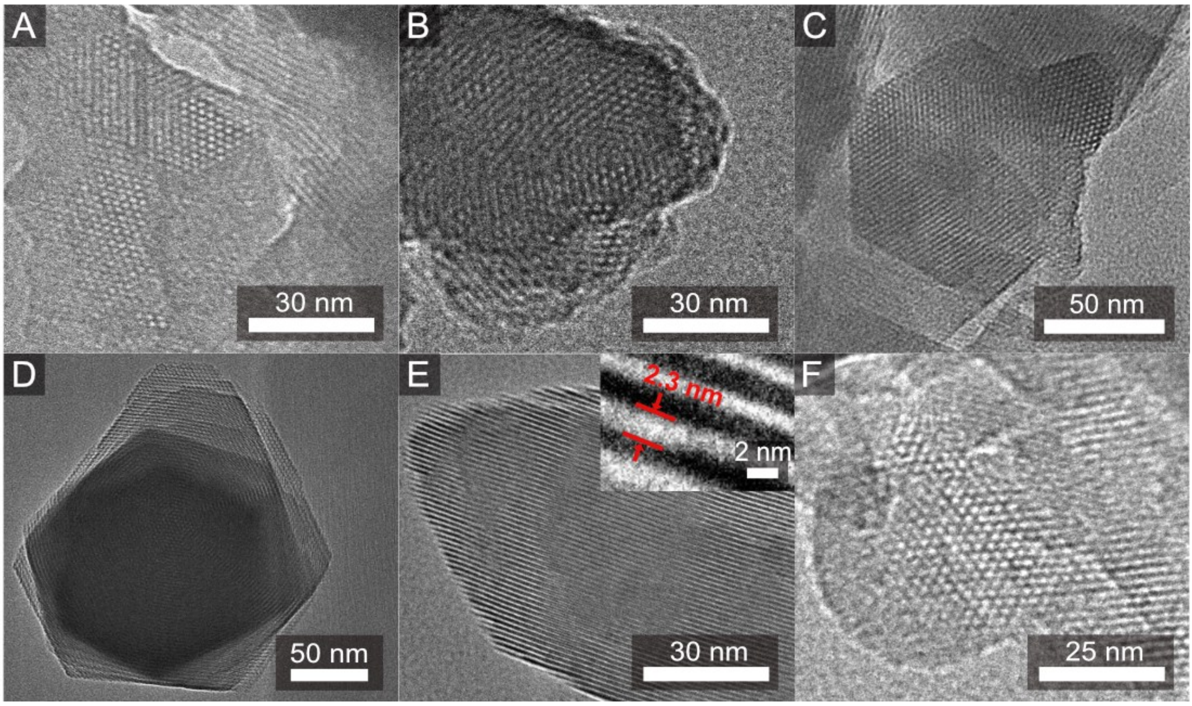

**F**

**igure S3**: High resolution TEM images of the ANMOF-74(M) series in [001] orientation showing **(A)** the Zn-, **(B)** Mg-, **(C)** Ni-, **(D)** Co-, **(F)** Mn-ANMOF-74 materials, respectively. **(E)** High resolution TEM image of ANMOF-74(Co) in side view showing a close-up of the lattice planes as inset.

## UV-VIS spectroscopy and photoluminescence of the ABHB linker

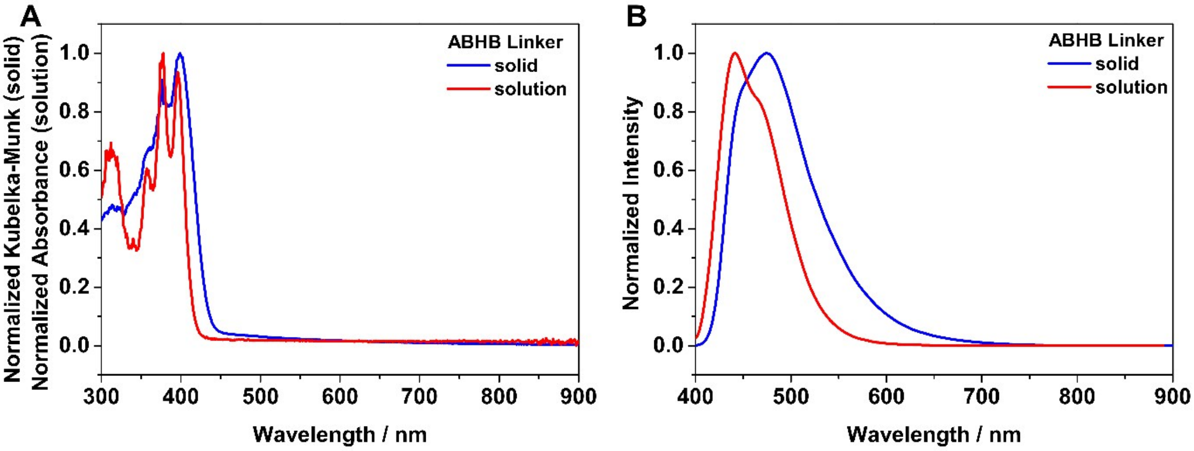

**Figure S4**: **(A)** Comparison of the absorption and diffuse reflectance spectra of the ABHB linker in $CHCl_3$ solution (red) and as solid dispersed in $BaSO_4$ (blue). **(B)** PL spectra of the ABHB linker measured with pulsed 378 nm excitation in $CHCl_3$ solution (red) and as solid (blue).

## Tauc plots of the ANMOF-74 series

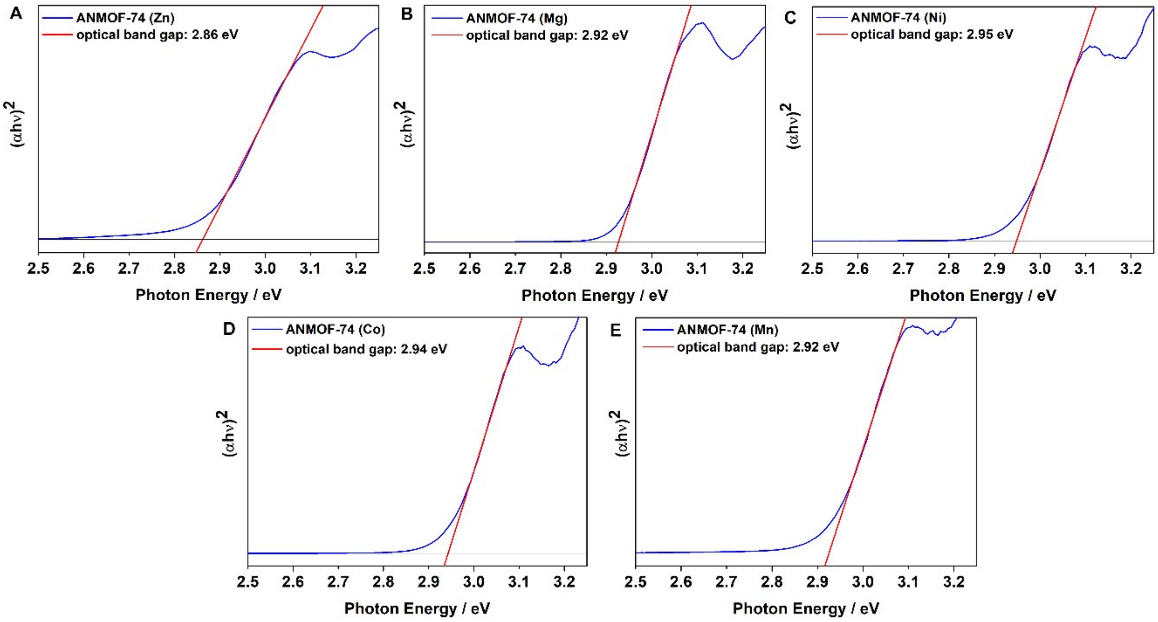

**Figure S5**: Tauc plots of ANMOF-74(Zn) **(A)**, ANMOF-7(Mg) **(B)**, ANMOF-74 (Ni) **(C)**, ANMOF-74(Co) **(D)** and ANMOF-74(Mn) **(E)**, suggesting the presence of direct band gaps.

## Time-correlated single photon counting (TCSPC) traces

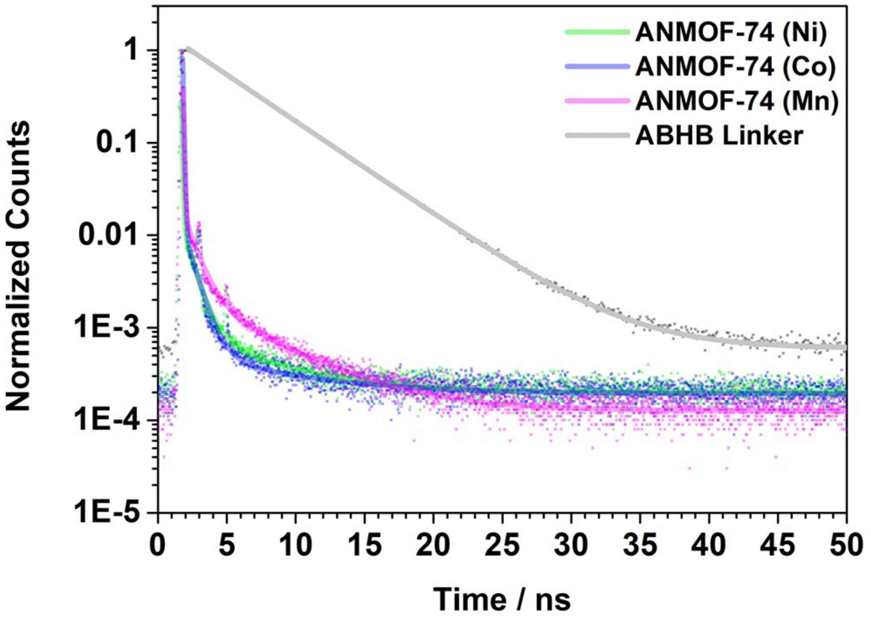

**Figure S6**: The time-correlated single photon counting (TCSPC) traces corresponding to the PL spectra of ANMOF-74(Ni), ANMOF-74(Co) and ANMOF-74(Mn) as solids and of the ABHB linker in solution which were recorded at the respective emission maximum of each material. The solid lines represent the exponential fits.

**Table S1**: The PL lifetimes (τ) of the ANMOF-74(M) series and of the ABHB linker, obtained from triexponential fits (see Figure S5 and 6) the TCSPC traces of the MOFs and from a monoexpontial fit of the TCSPC trace of the ABHB linker, as well as the error and the fractional intensities in percentages, which are the fractions of emitted photons corresponding to the respective lifetimes. We note that the stated error is the fitting error and that it does not necessarily reflect the actual resolution of the setup of around 100 ps.

| **sample** | | **τ / ns** | **error / ns** | **fractional intensity / %** |
|---|---|---|---|---|
| ANMOF-74 (Zn) | $\tau_1$ | 0.162 | ±0.012 | 22.9 |
| | $\tau_2$ | 0.79 | ±0.03 | 59.5 |
| | $\tau_3$ | 3.4 | ±0.2 | 17.6 |
| ANMOF-74 (Mg) | $\tau_1$ | 0.169 | ±0.006 | 28.7 |
| | $\tau_2$ | 1.03 | ±0.02 | 50.0 |
| | $\tau_3$ | 4.90 | ±0.12 | 21.3 |
| ANMOF-74 (Ni) | $\tau_1$ | 0.065 | ±0.004 | 55.3 |
| | $\tau_2$ | 0.80 | ±0.06 | 31.9 |
| | $\tau_3$ | 5.6 | ±1.0 | 12.8 |
| ANMOF-74 (Co) | $\tau_1$ | 0.064 | ±0.002 | 80.5 |
| | $\tau_2$ | 0.79 | ±0.06 | 15.5 |
| | $\tau_3$ | 7 | ±2 | 4.0 |
| ANMOF-74 (Mn) | $\tau_1$ | 0.065 | ±0.003 | 48.3 |
| | $\tau_2$ | 0.89 | ±0.06 | 28.8 |
| | $\tau_3$ | 5.1 | ±0.4 | 22.9 |
| Anthracene (Monomer) | τ | 4.32 | ±0.011 | 100 |

## Photoluminescence quantum yield (PLQY) and CIE color space

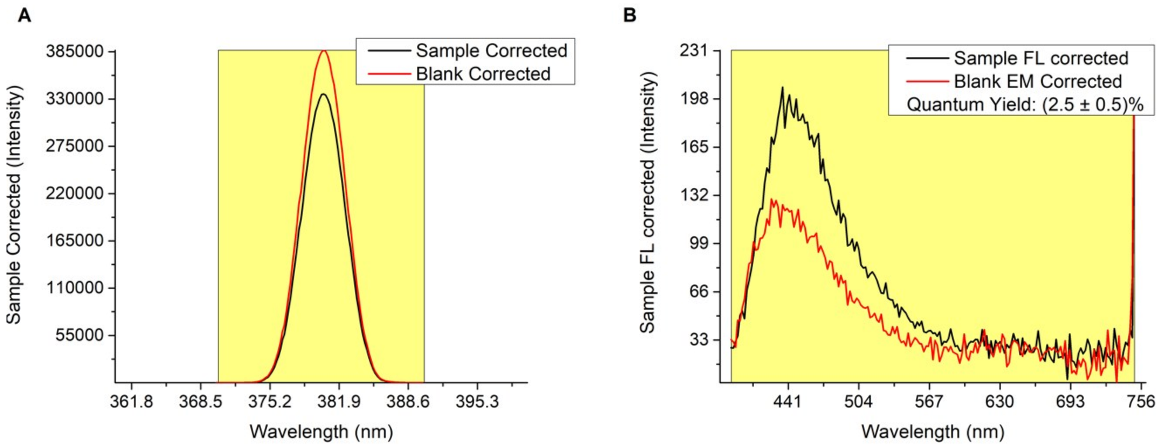

**Figure S7**: Photoluminescence quantum yield (PLQY) measurement of ANMOF-74(Mg). Rayleigh peak (A) and emission (B) data with integration boundaries.

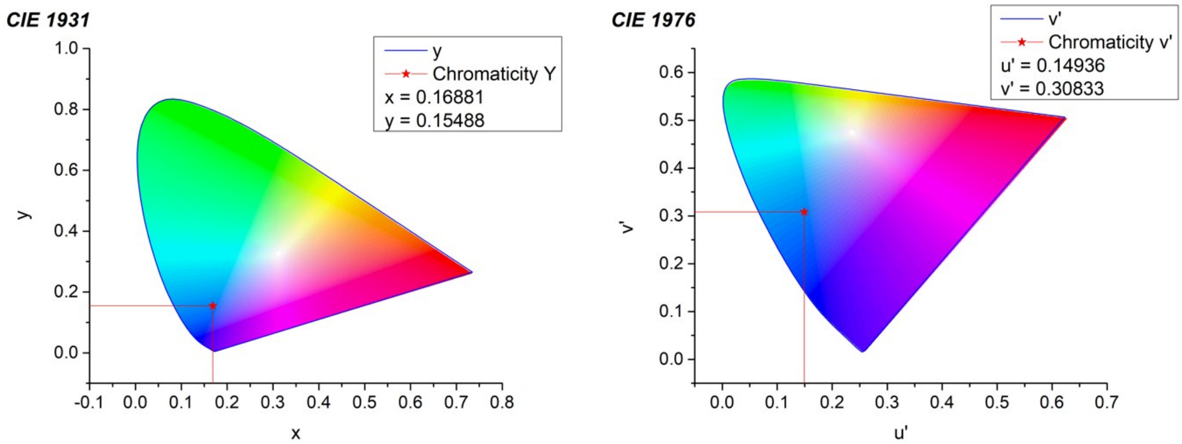

**Figure S8**: CIE 1931 and CIE 1976 color spaces with the ANMOF-74(Mg) emission and the respective coordinates.

**Figure S9**: Photo image of a ANMOF-74(Mg) pellet during irradiation with a 365 nm wavelength.

## Thermogravimetric analysis (TGA) of the ANMOF-74 series

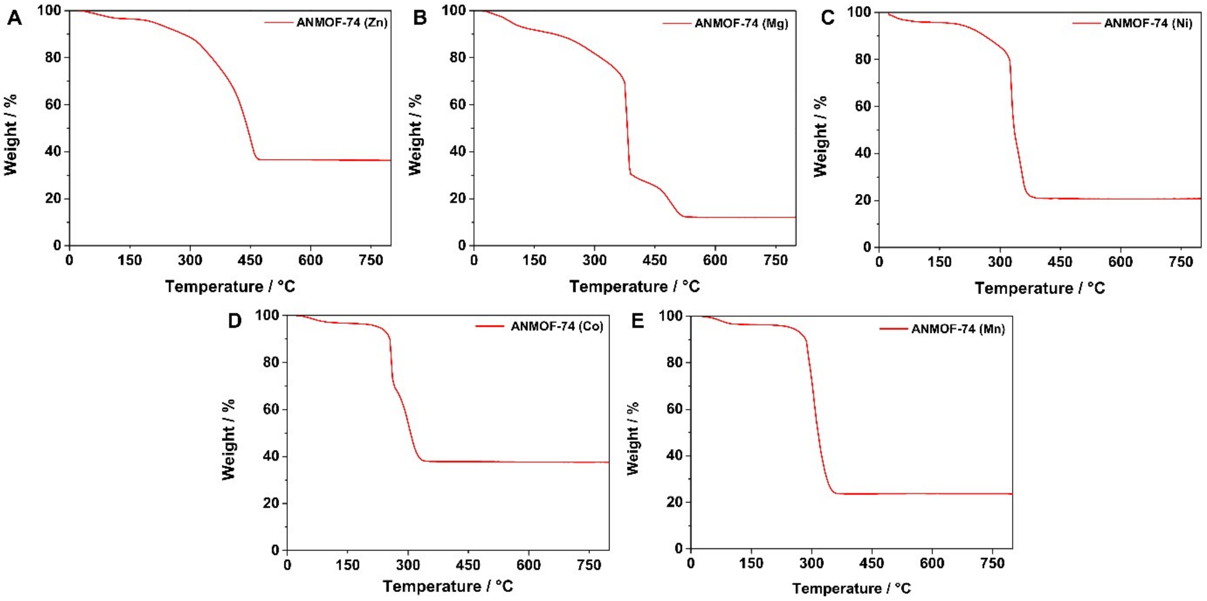

**Figure S10**: Thermogravimetric Analysis (TGA) of (**A**) ANMOF-74(Zn), (**B**) ANMOF-74(Mg), (**C**), ANMOF-74(Ni), (**D**) ANMOF-74(Co) and (**E**) ANMOF-74(Mn) measured as bulk materials (20 mg).

## Energy dispersive X-ray (EDX) spectra of ANMOF-74 (M)

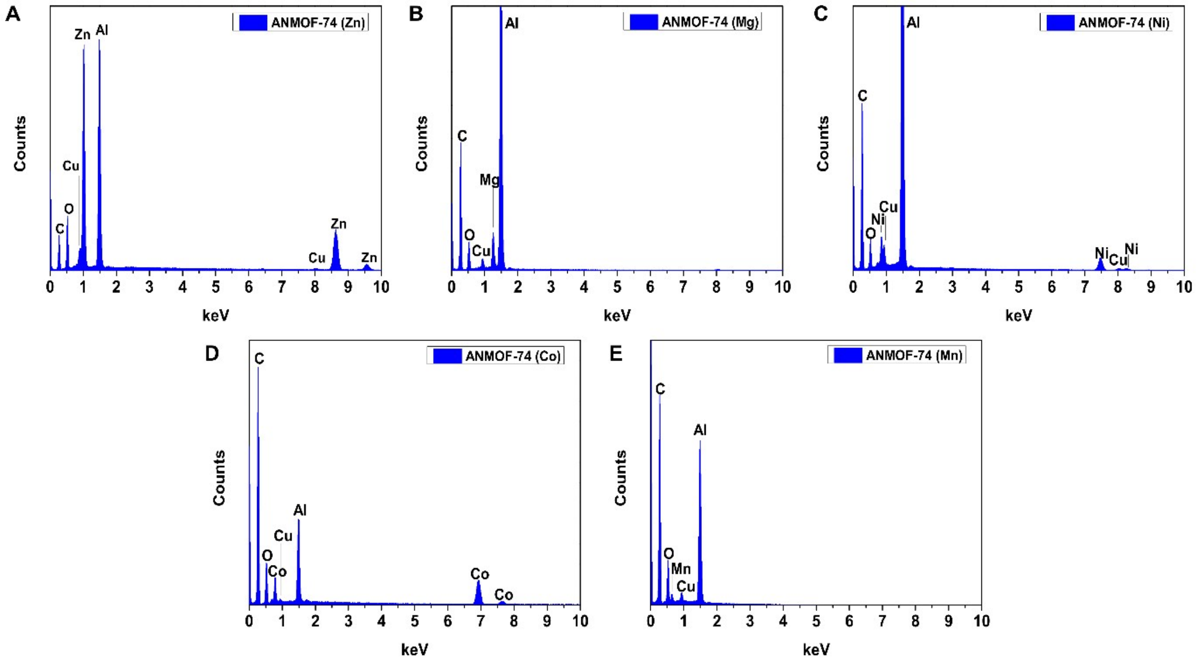

**Figure S11**: Energy dispersive X-ray (EDX) spectra of (**A**) ANMOF-74(Zn), (**B**) ANMOF-74(Mg), (**C**), ANMOF-74(Ni), (D) ANMOF-74(Co) and (**E**) ANMOF-74(Mn), measured as bulk materials on an SEM sample holder.

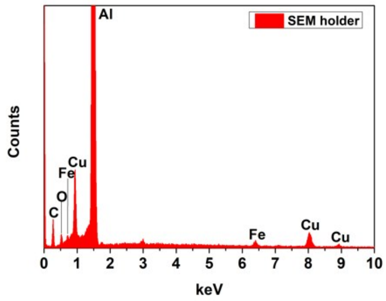

**Figure S12**: Energy dispersive X-ray (EDX) spectrum of the SEM sample holder.

## X-ray photoelectron spectroscopy (XPS) of the ANMOF-74 series

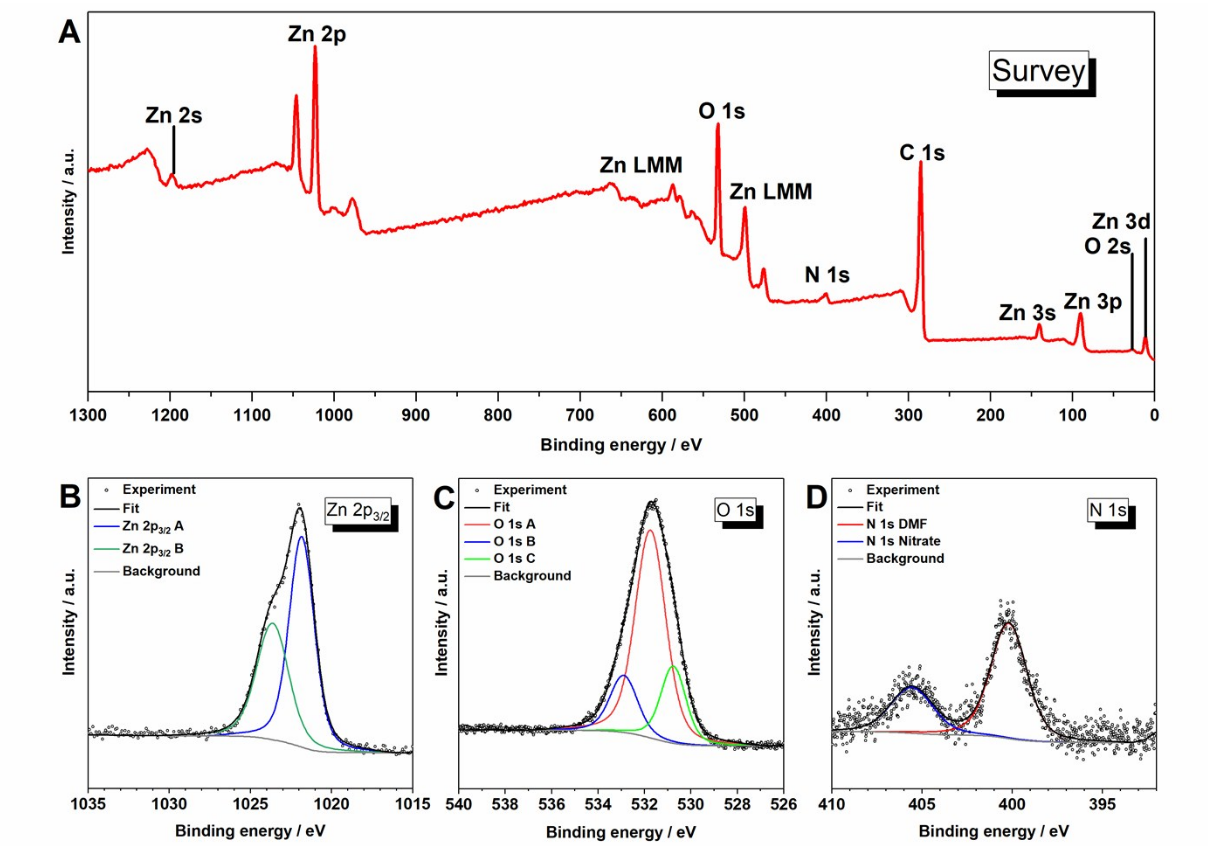

**Figure S13**: XPS spectra of ANMOF-74(Zn) powder: (**A**) survey scan, (**B**) Zn 2p spectrum, (**C**) O 1s spectrum and (**D**) N 1s spectrum.

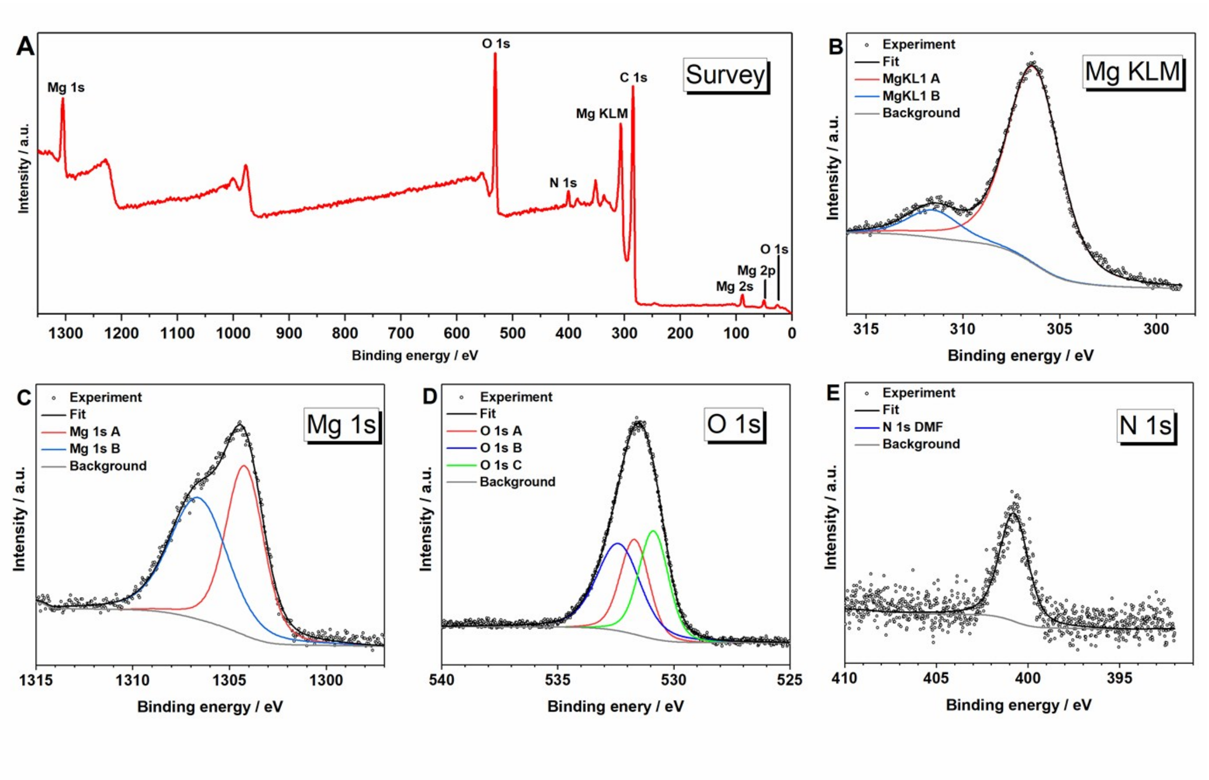

**Figure S14**: XPS spectra of ANMOF-74(Mg) powder: (**A**) survey scan, (**B**) Mg KLM spectrum, (**C**) Mg 1s spectrum, (**D**) O 1s spectrum and (**E**) N 1s spectrum.

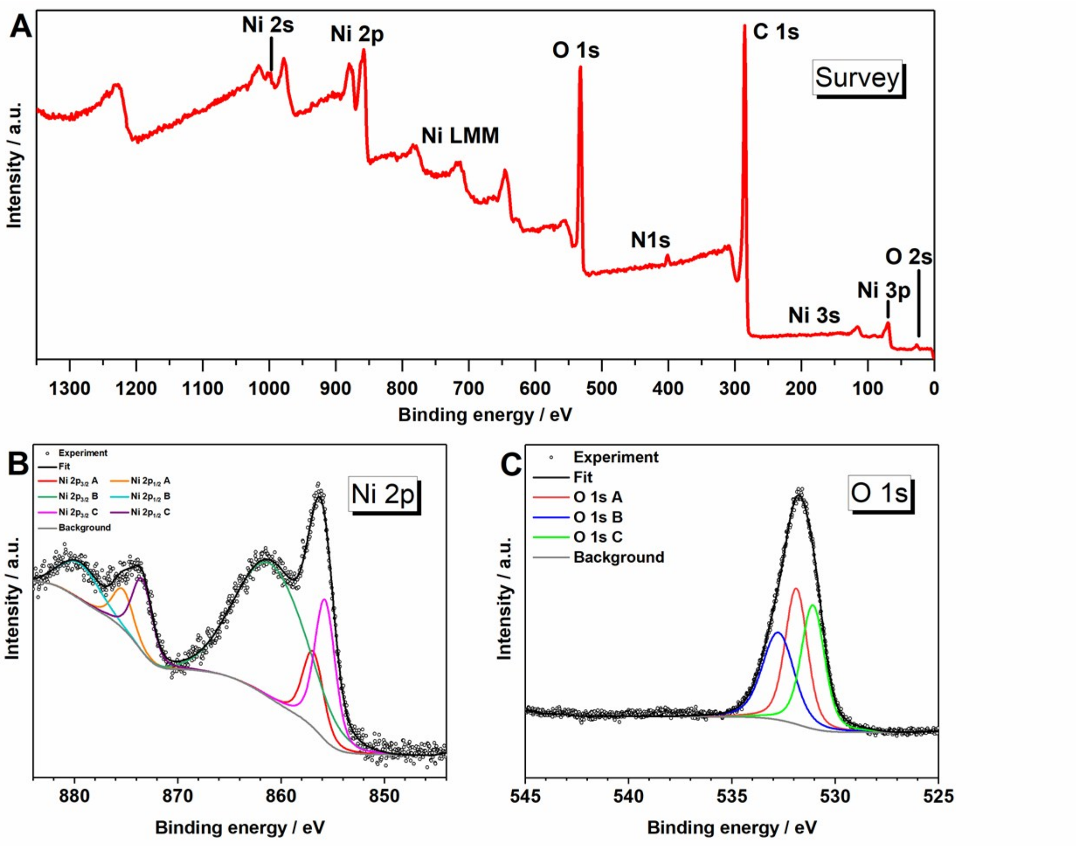

**Figure S15**: XPS spectra of ANMOF-74(Ni) powder: (**A**) survey scan, (**B**) Ni 2p spectrum and (**C**) O 1s spectrum.

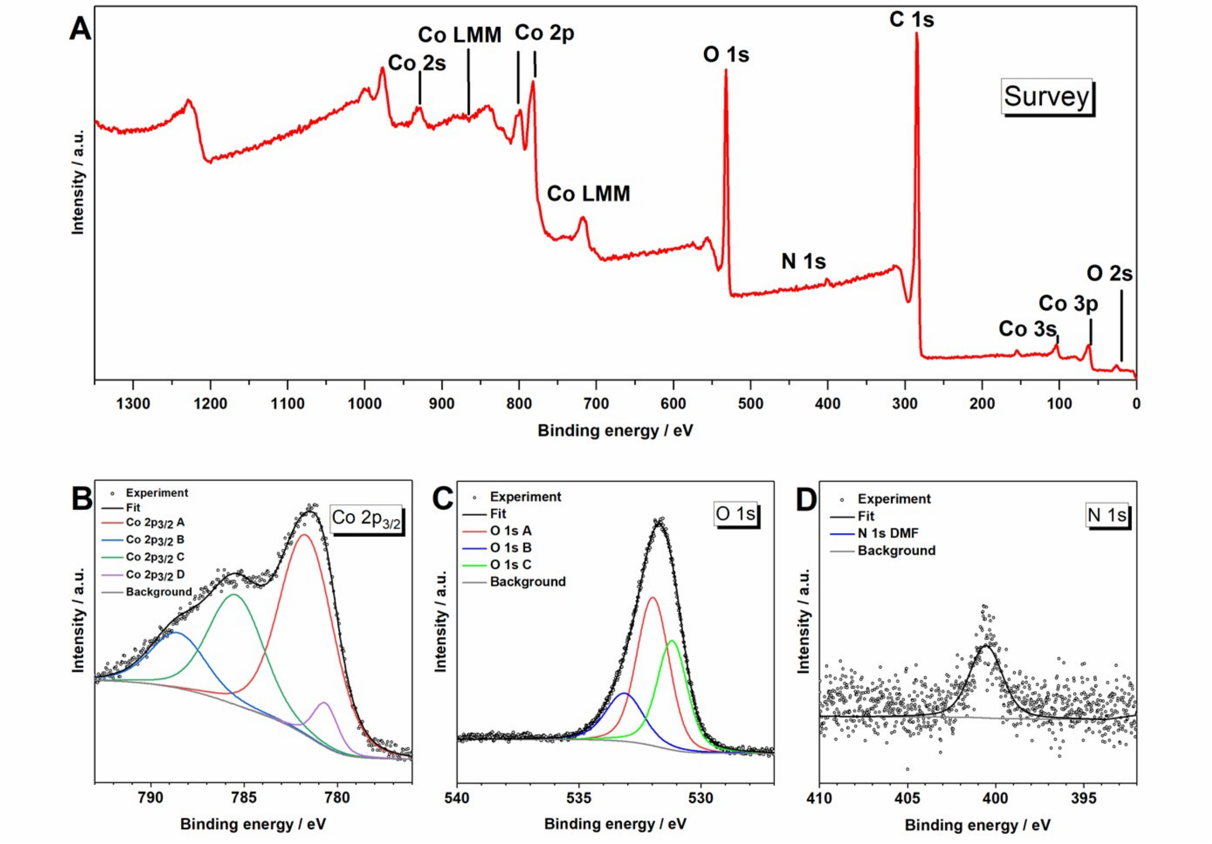

**Figure S16**: XPS spectra of ANMOF-74(Co) powder: (**A**) survey scan, (**B**) Co 2p spectrum, (**C**) O 1s spectrum and (**D**) N 1s spectrum.

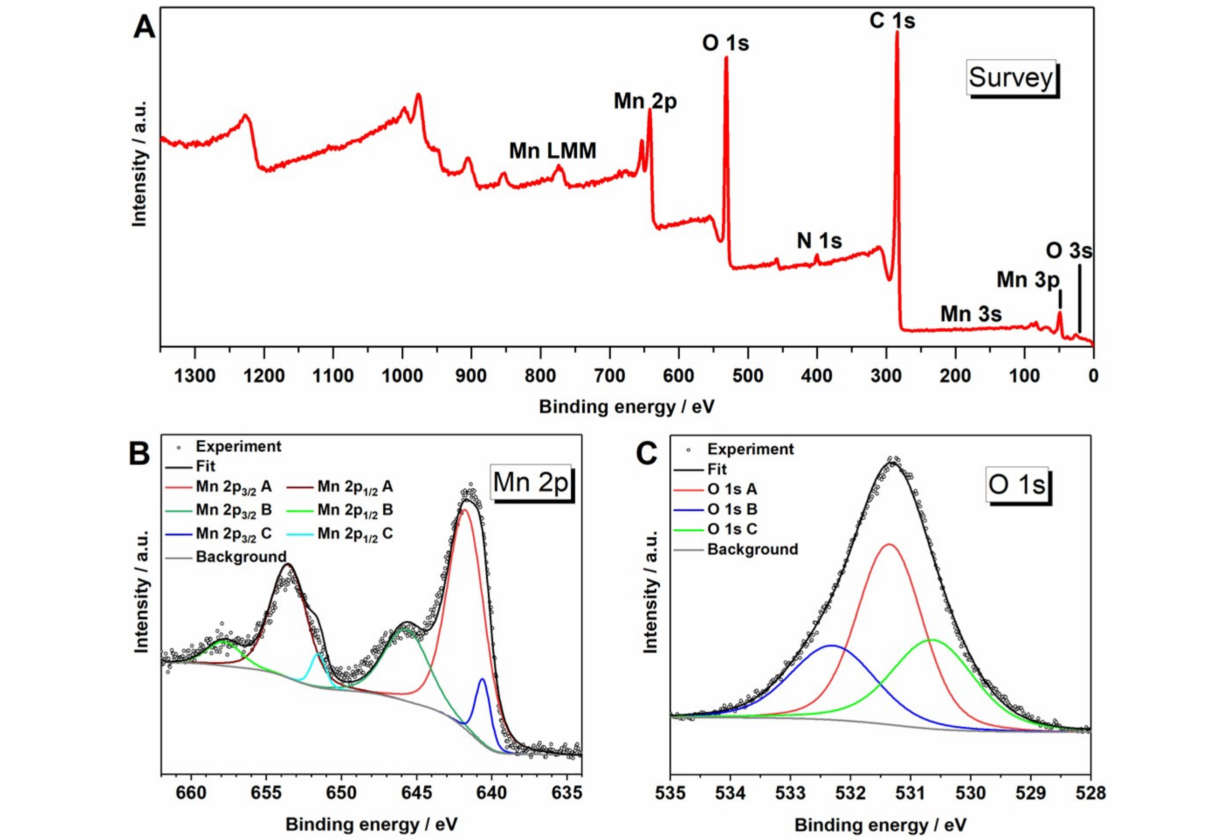

**Figure S17**: XPS spectra of ANMOF-74(Mn) powder: (**A**) survey scan, (**B**) Mn 2p spectrum and (**C**) O 1s spectrum.